Published in final edited form as:
Glia. 2012 December ; 60(12): 1906–1914. doi:10.1002/glia.22406.

Regulation of serum response factor by miRNA-200 and miRNA-9 modulates oligodendrocyte progenitor cell differentiation

Benjamin Buller[1], **Michael Chopp**[1,3], **Yuji Ueno**[1], **Li Zhang**[1], **Rui Lan Zhang**[1], **Daniel Morris**[2], **Yi Zhang**[1], and **Zheng Gang Zhang**[1]

[1]Department of Neurology, Henry Ford Hospital, Detroit, MI, USA

[2]Department of Emergency Medicine, Henry Ford Hospital, Detroit, MI, USA

[3]Department of Physics, Oakland University, Rochester, MI, USA

Abstract

Serum response factor (SRF) is a transcription factor that transactivates actin associated genes, and has been implicated in oligodendrocyte (OL) differentiation. To date, it has not been investigated in cerebral ischemia. We investigated the dynamics of SRF expression after stroke *in vivo* and the role of SRF in oligodendrocyte differentiation *in vitro*. Using immunohistochemistry, we found that SRF was upregulated in OLs and OL precursor cells (OPCs) after stroke. Moreover, upregulation of SRF was concurrent with downregulation of the microRNAs (miRNAs) miR-9 and the miR-200 family in the ischemic white matter region, the corpus callosum. Inhibition of SRF activation by CCG-1423, a specific inhibitor of SRF function, blocked OPCs from differentiating into OLs. Over-expression of miR-9 and miR-200 in cultured OPCs suppressed SRF expression and inhibited OPC differentiation. Moreover, co-expression of miR-9 and miR-200 attenuated activity of a luciferase reporter assay containing the *Srf* 3′ untranslated region (UTR). Collectively, this study is the first to show that stroke upregulates SRF expression in OPCs and OLs, and that SRF levels are mediated by miRNAs and regulate OPC differentiation.

INTRODUCTION

Stroke is the most common disease of the central nervous system (CNS), and is the leading cause of permanent disabilities in the United States. Currently, stroke patients face disparaging odds that they will overcome their lingering neurologic deficits. Oligodendrocytes (OLs), the progeny of OL precursor cells (OPCs), are the only myelinating cells in the CNS. They are particularly sensitive to ischemic injury (Pantoni et al., 1996, Lyons and Kettenmann, 1998), and death of OLs leads to loss of myelin in the brain and ultimately impairment of neurologic function (Zhang et al., 2009, McIver et al., 2010, Chida et al., 2011). We have previously shown that enhancement of axonal outgrowth and myelination in the ischemic boundary zone (IBZ) leads to improved functional outcomes in a rat model of stroke (Liu et al., 2010, Zhang et al., 2010, Ueno et al., 2012). The IBZ is the area that is adjacent to the infarcted area, and this tissue may be salvageable after stroke. Furthermore, therapies promoting proliferation of OPCs, remyelination, or

To whom correspondence should be addressed: Zheng Gang Zhang, MD, PhD, Department of Neurology, Education & Research Building, #3056, Henry Ford Hospital, 2799 West Grand Boulevard, Detroit, MI 48202, USA, Office: (313) 916-5456, Fax: (313) 916-1318, zhazh@neuro.hfh.edu.

The authors have no conflicts of interest to declare.

white matter remodeling correlate with positive neurologic outcomes (Li et al., 2006, Shen et al., 2006).

In the present study, we investigated the dynamics and molecular interactions of serum response factor (SRF)—a widely expressed transcription factor—after stroke *in vivo* and *in vitro*. SRF is a ubiquitous transcription factor that has homologs in organisms as disparate as mammals, plants and fungi (Shore and Sharrocks, 1995, Riechmann and Meyerowitz, 1997, Herdegen and Leah, 1998). SRF directly transactivates over 200 genes, including actin, and it has been implicated in axonal outgrowth, pathfinding, and growth cone collapse (Knoll et al., 2006). Recently, it was shown that expression of SRF in neurons promotes OPCs to differentiate to mature OLs (Stritt et al., 2009). However, the effect of SRF expression in OLs or OPCs has not been thoroughly investigated.

Discovered recently, microRNAs (miRNAs) are short non-coding RNAs, typically about 20 nucleotides long. They suppress translation by binding to the 3′ untranslated region (3′UTR) of target mRNAs in a complementarity dependent manner. To date, it has not been shown whether any miRNAs directly regulate SRF in the CNS. Here, we show that SRF is activated in response to stroke in OPCs and OLs. *In vitro*, SRF promotes primary cultured OPCs to differentiate, and is regulated upstream by miR-9 and the miR-200 family. These novel data uncover a possible molecular target for enhancing the myelination of newly generated axons after stroke, a strategy that may aid in recovery.

MATERIALS AND METHODS

Ethics statement

The use and care of all animals employed in each of our experiments were approved by the Henry Ford Health System Institutional Animal Care and Use Committee, in accordance with all applicable laws and ethics standards.

Middle cerebral artery occlusion (MCAo) model

Male Wistar rats weighing 350 to 450 g were subjected to permanent right MCAo, as previously described (Chen et al., 1992). Briefly, the animals were anesthetized with 4% isoflurane during induction and then maintained with 1% isoflurane in a mixture of 30% O_2 and 70%N_2O. Body temperature was monitored and maintained at 37°Cusing a feedback-regulated water heating system. Under the operating microscope (Carl Zeiss), the right common carotid artery (CCA), the right external carotid artery (ECA), and the internal carotidartery (ICA) were isolated via a midline incision. A nylon suture was then advanced from the ECA into the lumen of the ICA until it reached the origin of the MCA, approximately 17 to 18 mm. The ECA was then ligated and the incision closed.

Tissue Processing and Immunostaining

Rats were sacrificed at 4 hours and 1, 2, 4, 7 or 14 days (d) after MCAo (3 rats per group), and perfused with heparinized saline followed by 4% paraformaldehyde (PFA) via a needle inserted into the left ventricle. The brains were removed, fixed in 4% PFA for 2d, and then embedded in paraffin. The brains were cut coronally in 6μm sections, and mounted on slides for analysis. For immunohistochemistry, the brain sections were fixed in 4% PFA, blocked in PBS with 1% bovine serum albumin (BSA), and incubated with monoclonal antibodies against the following proteins: 2′,3′-cyclic nucleotide 3′ phosphodiesterase (CNPase; 1:250; Aves Labs); microtubule associate protein 2 (MAP2; 1:200; Millipore); adenomatous polyposis coli (APC; 1:20; GenWay Biotech); and a polyclonal antibody against SRF (1:75; Abcam). For immunocytochemistry, cells were plated onto 8 well chamber slides at desired concentrations and were incubated with anti-CNPase (1:500) and myelin basic protein

(MBP; 1:500; Millipore; monoclonal) after fixation and blocking. Fluorescently labeled secondary antibodies were used to visualize proteins. All sections and cells were counterstained with 4′,6-diamidino-2-phenylindole (DAPI; 1:10,000) to visualize nuclei.

Isolation of Total RNA and Real-Time RT-PCR

To analyze miRNA both *in vivo* and *in vitro*, cells were lysed in Qiazol reagent and total RNA was isolated using the miRNeasy Mini kit (Qiagen). Brain sections were used for *in vivo* miRNA analysis. Before isolation, sections were deparaffinized with xylene and rinsed twice in 95% ethanol to remove xylene. They were then treated with proteinase K for 10min to remove crosslinks between proteins and RNA, and then the corpus callosum was dissected out and lysed in Qiazol. MiRNA was reverse transcribed with the miRNA Reverse Transcription Kit (Applied Biosystems) and amplified with TaqMan miRNA assays (Applied Biosystems), which are specific for mature miRNA sequences. To determine relative gene expression, the $2^{-\Delta\Delta Ct}$ method was used (Livak and Schmittgen, 2001).

Cell Culture and Transfection

For *in vitro* experiments, primary OPCs were isolated using a method from a published protocol (Chen et al., 2007), which we have modified to accommodate embryonic day (ED) 18 rat embryos. Briefly, pregnant Wistar rats were decapitated under deep anesthesia and a c-section was performed. The scalp and meninges were removed and cortices were dissected out. Cortices were then rinsed twice in ice-cold Hank's buffered salt solution (HBSS) and incubated at 37°C for 15 min with 0.01% trypsin and DNase. The tissue was then triturated and filtered through a 40μm sterile cell strainer to remove insoluble debris. Cells were plated in poly-D-lysine coated T75 culture flasks in DMEM with 20% FBS until the cells were confluent (~10 days), in which time a bed of astrocytes grew with a layer of OPCs on top. The flasks were then shaken at 200 RPM for one hour to dislodge dead cells and microglia; the media were then changed, and the flasks shaken over night at 200 RPM to dislodge OPCs. The OPCs were collected and plated onto poly-D, L-ornithine coated culture dishes with serum free DMEM supplemented with hormones and growth factors (10 nM each platelet-derived growth factor-alpha [PDGF-AA] and basic fibroblast growth factor [bFGF]). To induce differentiation, growth factors were withdrawn from the medium and cilliary neurotrophic factor (CNTF) added. To avoid spontaneous differentiation, cells were not used beyond one passage.

For transfection and luciferase experiments, we employed N20.1 cells, an immortalized mouse OPC line that differentiates when the incubation temperature is raised to 39°C (Paez et al., 2004). N20.1 cells were differentiated for 8d, which we have previously shown to be an appropriate length of time to express maturity markers (Zhang et al., 2008). N20.1 cells were generously provided by Dr. Anthony Campagnoni, University of California at Los Angeles, and cultured in DMEM with 10% FBS, antibiotics and supplemented with dextrose. Cells were maintained under G418 antibiotic selection to ensure a pure culture and passaged when they became ~95% confluent. To overexpress miR-9 and miR-200b, miRIDIAN miRNA mimics (Dharmacon) were transfected into N20.1 cells via Lipofectamine 2000 reagent (Invitrogen) according to the manufacturer's instructions. A mimic of miR-67, which is not expressed in mammals, was used as control.

Western Blotting

Cells were lysed in radioimmunoprecipitation (RIPA) buffer containing protease inhibitors; the lysate was sonicated, then centrifuged for 10 min at $>2 \times 10^4$g to remove cell debris. When necessary, cytoplasmic and nuclear proteins were separated with NE-PER Nuclear and Cytoplasmic Extraction Reagents (Thermo Scientific). Protein concentrations were determined using a bicinchoninic acid (BCA) assay (Thermo Scientific). Equal amounts of

protein were then separated by SDS-PAGE and transferred to a nitrocellulose membrane. Membranes were probed with 1o antibodies against SRF (1:500), MBP (1:1000), NG2 proteoglycan (1:1000; Millipore; monoclonal), PDGF receptor (PDGFR; 1:1000; Santa Cruz; polyclonal) or β-Actin (1:10000; Abcam; monoclonal), followed by 2o antibodies against mouse (β-Actin), rabbit (SRF, NG2, PDGFR) or rat (MBP) conjugated to horseradish peroxidase. Proteins were visualized by enhanced chemiluminescence. Relative intensities were determined by use of ImageJ software.

Target Prediction

The software packages TargetScan5.1 (targetscan.org), miRanda (microrna.org), and PicTar (pictar.mdc-berlin.de) were consulted to search for putative miRNA regulators of SRF. Highly conserved binding sites, as well as binding sites for miRNAs that were known from literature reports to have a role in OPC maturation were considered for study.

Luciferase Activity Assay

DNA encoding a segment of the *Srf* 3′UTR was cloned into the pMiR Report luciferase vector. Two vectors were synthesized. One contained a 60 base pair segment encompassing the lone miR-200 binding site. The other contained a 600 base pair segment that encompassed the miR-9 binding site, as well as the miR-200 binding site proximal to it. Point mutations were designed to make binding energetically unfavorable. Mutagenesis was outsourced (Genscript), and each mutation was confirmed by sequencing. Each vector was transfected intoN20.1cells by Lipofectamine 2000 reagent. Luciferase activity and transfection efficiency are higher in N20.1 cells than primary cultured OPCs; they are therefore more suitable for use in luciferase activity assays. Luciferase activity was determined by the Luciferase Assay System (Promega) on a microplate reader (Perkin Elmer).

Statistics

The data are presented as mean ± s.e. One way ANOVA was used for multiple group experiments. Ad hoc two sample t-tests were used for two-group comparisons. A value of $P<0.05$ was taken as significant.

RESULTS

Expression of SRF in the brain after stroke

SRF has been reported to be upregulated in some cell types after acute ischemia (Lu et al., 2009). Consistent with these reports, double immunostaining revealed immunoreactivity of SRF in MAP2 positive neurons of the cortical IBZ 4h after MCAo (38 ± 8%, mean ± S.D.; n=3). Expression of SRF in neurons remained robust for 1d, with 47 ± 12% of cortical IBZ neurons showing SRF reactivity (n=3). However, 2d after MCAo and thereafter, neuronal expression of SRF was markedly decreased, with only 8 ± 2% of IBZ neurons positive for SRF (n=3; $P<0.01$ vs. 4h or 1d; Fig. 1A, B, E). After 2d, SRF expression was negligible in neurons. Conversely, SRF reactivity in CNPase (a marker of maturing OLs) reactive cells dramatically increased after stroke in the same cohort. Initially, at 4 hours, only 6 ± 6% of CNPase+ cells were reactive for SRF. By 14 days after stroke, 64 ± 6% of CNPase+ cells also were SRF+ ($n = 3$; $P < 0.001$; Fig. 1C–E). Additionally, we measured the co-expression of SRF with APC—a marker of mature OLs—at acute and chronic times after stroke. At 4h after ischemia, we did not observe any colocalization of SRF with APC in the ipsilateral or contralateral hemispheres, in either white or grey matter. However, at 14d after stroke many APC reactive cells of the ischemic boundary zone expressed SRF (Fig. 1F), although no colocalization was observed in the contralateral hemisphere. Most notably, we observed

clusters of APC positive cells among which one or two constituents expressed SRF, suggesting that SRF transiently expresses during maturation of OLs, and that its expression may be lost after full maturation. These data suggest, therefore, that SRF is associated with differentiation of OPCs to OLs after stroke.

SRF mediates differentiation of OPCs in vitro

Based on our *in vivo* data, we hypothesized that SRF promotes OPCs to differentiate into OLs. To test the biologic function of SRF, we employed a primary culture model of OPCs from E18 rat embryos. Morphologically, the cells changed from having a few long processes to many short, highly branched processes typical of mature OLs when the cells were switched from growth medium (GM) to differentiation medium (DM), immunofluorescent staining revealing that these cells were MBP positive cells with stereotypical myelin sheets (Fig. 2A–C). Quantification of MBP reactive cells revealed that only 7% of cells were reactive for MBP when grown in GM, indicating a high percentage of OPCs. However, the proportion of MBP reactive cells increased to 42% and 82% after 2d and 4d, respectively, in DM. Furthermore, Western blot confirmed that 4d of differentiation drastically increased MBP expression while decreasing expression of immature OPC markers NG2 and PDGF-AA receptor (PDGFR; Fig. 2D). These data indicate that our primary OPCs differentiate into OLs, which is consistent with other published studies that have used this method (Chen et al., 2007, Hayakawa et al., 2011). Therefore, we used the primary OPCs to investigate the role of SRF in OL differentiation. Immunocytochemistry analysis revealed that 18 ± 2% of OPCs grown in GM were reactive for SRF, which was primarily localized to the cellular processes. In contrast, after 2d in DM, the proportion of SRF positive cells increased to 62 ± 5%, with expression subsiding slightly to 46 ± 4% by 5d in DM ($P < 0.05$; Fig. 2E–H). SRF immunoreactivity was highly observed in the nucleus in DM, although it was also strong in the processes in 2d-DM cells. Consistent with Immunocytochemistry results, Western blot analysis showed that SRF was upregulated by 1.8± 0.2 fold ($n = 3$; $P < 0.05$; Fig. 2I, J) after 4d of differentiation. These *in vitro* data suggest that SRF expression is associated with maturation of OLs, which is in agreement with our *in vivo* data. We then examined the role of SRF in primary OPC differentiation by blocking SRF with CCG-1423. CCG-1423 is a molecule that specifically inhibits the function of SRF at a concentration of 300nM (Evelyn et al., 2007). We found that at this concentration CCG-1423 significantly suppressed elevation of MBP levels measured by Western blots when OPCs were cultured in DM (Fig. 2I, J), suggesting that inhibition of SRF activity is sufficient to arrest differentiation of OPCs. Addition of CCG-1423 to DM did not significantly alter SRF expression. We next separated nuclear and cytoplasmic protein from cells that had been incubated in normal DM, or DM with CCG-1423, and measured phosphorylated (active) SRF. We found that the level of cytoplasmic p-SRF was unaltered in cells incubated with CCG-1423 compared to normal DM. However, while p-SRF was evident in the nuclei of normally differentiated cells, we did not detect it in the nuclei of CCG-1423 cells (Fig. 2K). These data support a role for SRF in promoting differentiation of OPCs.

miR-9 and miR-200bare suppressed in white matter after stroke

The dynamical expression of SRF after stroke led us to hypothesize that SRF may be translationally regulated. To determine if miRNAs are involved in mediating the SRF expression, we consulted the software packages TargetScan, miRanda and PicTar to perform an *in silico* analysis; each identified the miR-200 family (encompassing miR-200b, miR-200c and miR-429) as a potential regulator of SRF, with two available binding sites in the *Srf* mRNA 3′UTR. Additionally, TargetScan identified a single binding site in the *Srf* 3′UTR for miR-9. Despite only one of three programs identifying a miR-9 binding site, we focused on it because it is expressed in all CNS cell types, is highly expressed in OLs, and

was shown to be specifically downregulated during differentiation of OPCs to OLs (Smirnova et al., 2005, Lau et al., 2008).

To determine expression of miR-200 family and miR-9 in white matter after stroke, we dissected the portion of the corpus callosum whose blood supply is mainly carried by the MCA from animals 4h or 14d after MCAo. White matter tracts are enriched in OLs, and we observed them to highly express SRF after stroke. Thus, we reasoned that measuring expression of miR-9 and -200 in the corpus callosum would provide a good estimate of their expression in OLs. At 14d of MCAo, expression of miR-9 and miR-200b were 34 ± 4% and 28 ± 4% as abundant compared to expression in the same area at 4h of MCAo ($n = 5$; $P < 0.05$; Fig. 3A). Therefore, expression of miR-9 and miR-200b in white matter had an inverse trend to expression of SRF in OPCs and OLs of the ischemic boundary after stroke; SRF, as mentioned above, was expressed in 6% of CNPase reactive cells initially after stroke, and increased to 64% 14d hence. We did not detect miR-200c to have significantly different expression at 4h and 14d, although its expression was abundant in each animal. Additionally, miR-429 expression was not significantly different at any time point, and its expression was detected to be low in each experiment. Based on these data, we conclude that down-regulation of miR-9 and miR-200b in the corpus callosum is specific after stroke.

miR-9 and miR-200 suppress SRF *in vitro*

We then investigated whether miR-9 and miR-200 regulate SRF expression, leading to OPC differentiation *in vitro*. We first measured miR-9 and miR-200 expression in cultured primary OPCs after 4d of differentiation. MiR-9 was expressed 0.46 ± 0.08 fold of expression in OPCs grown in GM ($n = 3$; $P<0.05$; Fig. 3B). Interestingly, in contrast to our *in vivo* measurement, miR-200b was not detected in cultured OPCs. However, miR-200c was highly expressed in OPCs grown in GM, and its expression was reduced to 0.70 ± 0.17 ($n = 3$; $P<0.05$; Fig. 3B) fold in OPCs that were differentiated for 4 d. These data indicate that miR-9 and miR-200 are associated with differentiation of OPCs. MiR-200b and -200c have high sequence homology (they differ by one base), and their seed sequences are identical. Therefore, we speculate that expression of either should have similar consequences. With this assumption, we elected to further investigate the effect of overexpressing miR-9 and miR-200b, given that expression of miR-200b is altered in adult animals after stroke more highly and consistently, thus perhaps replicating the *in vivo* case more faithfully.

To investigate the effects of miR-9 and miR-200b expression on differentiation of OPCs, we transfected each into cultured N20.1 cells, given the relative ease with which they can be transfected compared to cultured primary OPCs. Western blot analysis revealed that miR-200b mimic decreased SRF protein levels by 63 ± 19% compared to SRF levels in cells transfected with miR-67 mimic ($n=3$; $P<0.05$; Fig. 3C), while miR-9 mimic only slightly decreased SRF protein expression ($p>0.05$). However, when miR-9 and miR-200b mimics were co-transfected, SRF was depleted by an even greater amount than transfection with miR-200b mimic alone (71 ± 2% compared with control; $n=3$; $P < 0.05$; Fig. 3C). To further assess the impact of miR-9 and miR-200b mimic on maturation of N20.1 cells, we measured the number of CNPase immunoreactive N20.1 cells after 8d of differentiation in cells that had been overexpressed with miR-9 only, miR-200b only, miR-9 and miR-200b, or miR-67 negative control. In DM, many N20.1 cells were CNPase positive after transfection with miR-67 (Fig. 3D). However, CNPase was significantly downregulated when miR-9 and -200b mimics were co-transfected (12 ± 4% positive vs. 34 ± 8% in control cells; $n=3$; $P<0.05$; Fig. 3D). No significant differences were detected in the number of CNPase positive cells between cells with miR-67 mimic and those transfected with either miR-9 or miR-200b alone. These data suggest that miR-9 and miR-200 suppress differentiation at least in part by blocking SRF expression.

To investigate whether SRF expression is attenuated by direct targeting of miR-9 and miR-200b, we designed two luciferase reporter plasmids, one containing the putative miR-9 binding site and the miR-200 site proximal to it (miR-9-luc), and another containing only the miR-200 site distal from the others (miR-200-luc; see Fig. 4A for configuration and sequences). We elected to use two separate plasmids because the entire 3′UTR is ~2.3kb, too long for optimal luciferase expression. First, we transfected N20.1 cells with miR-200-luc plasmid and divided the cells into two groups; one group was co-transfected with miR-67 negative control mimic and the other with miR-200b mimic, and we assayed their luciferase activity. We found that the luminescence of the miR-200b treated group was attenuated by 68 ± 10% compared to miR-67 treated cells ($n = 4$; $P < 0.01$; Fig. 4B). Next, we transfected N20.1 cells with miR-9-luc plasmid and divided the cells into 3 groups; one group was co-transfected with miR-67; one with miR-9; and one with miR-200b. Overexpression of miR-200b alone showed no significant change in luciferase activity ($n = 4$; $P < 0.45$). However, introduction of miR-9 into the cells downregulated the luciferase activity by 33 ± 11%, which is significant compared to miR-67 control ($n = 4$; $P < 0.05$).

To confirm binding of miR-9 and miR-200 to the *Srf* 3′UTR, we introduced mutations into each of the three putative binding sites. The putative binding site of each of our sites of interest is 7 nucleotides long. We chose to mutate the center base on each site in order to destabilize the bond. The middle base of the miR-200 binding site in the miR-200-luc plasmid was changed from U to A (U and A cannot form Wobble base pairs). The mutation was confirmed by sequencing. We then repeated each measurement described above. When miR-200b was introduced into miR-200-luc mutant vector containing cells, the luminescence was measured to be 87 ± 16% ($n = 4$; $P = 0.29$) compared to miR-67 expressing cells, suggesting that the mutation effectively eliminated binding of miR-200 to the putative site. We next introduced a mutation into the miR-9 site on the miR-9-luc vector and repeated the experiment. This binding site has an A as its middle base that was changed to U and confirmed by sequencing. After this mutation was introduced, miR-9 could no longer attenuate luciferase activity. Meanwhile, miR-200 still did not affect the luciferase activity. Next, we mutated the miR-200 binding site on the miR-9-luc vector. In this set of experiments, miR-9 retained its capacity to attenuate the assay activity, and was similar to the level of attenuation we measured in the wild-type assay (74 ± 22%; $n = 4$; $P < 0.05$; Fig. 4B), while miR-200 overexpression had no effect on luminescence. We therefore conclude that miR-9 and miR-200 each act to regulate expression of SRF by directly binding to the 3′UTR of the *Srf* gene.

DISCUSSION

The present study is the first to describe a direct role for SRF in the maturation of OLs, and the first to demonstrate upregulation of SRF and downregulation of miR-9 and miR-200b in OLs and white matter, respectively, after stroke. Furthermore, we have confirmed that miR-9 and miR-200 target the *Srf* 3′UTR. The observation that miR-9 targets *Srf* is a novel observation, and a potentially important one, given that miR-9 has previously been shown to be suppressed in differentiating OPCs (Smirnova et al., 2005, Lau et al., 2008). MiR-200c has been shown to disrupt expression of SRF in breast cancer cells, but active binding to the *Srf* transcript was not shown (Jurmeister et al., 2012). Several human studies demonstrated that functional improvement of motor and cognitive skills after stroke correlates with remodeling of white matter tracts and/or reorganization of cortical architecture (Saur et al., 2006, Buma et al., 2010, Wang et al., 2011), both of which require changes in myelination. Unsurprisingly then, therapies aimed at increasing the number of myelinating OLs in the IBZ have shown promise in mitigating functional deficits in experimental animal models of stroke (Morris et al., 2010, Zhang et al., 2010). Therefore, SRF may represent a novel

pharmacologic target for lessening functional impairment after stroke, via its effect on oligodendrocyte maturation.

SRF has been well studied in neurons of the CNS (for extensive review, see e.g. (Knoll and Nordheim, 2009)), but to date, a direct role for SRF has not been described in OPC/OLs. Our data show that upregulation of SRF correlates to maturation of OLs, and that when SRF is inhibited differentiation of OPCs is arrested. Thus, the present study indicates that overexpression of SRF promotes oligodendrocyte maturation. Since the original submission of our study, Lu and Ramanan have shown that knockout of *Srf* in nestin expressing neural progenitor cells causes a 50% reduction of OPCs in postnatal mice (Lu and Ramanan, 2012). Our data corroborate and add to their observation by showing that SRF is likely involved in the transition from early stage progenitor to mature OL, given that we observed the strongest colocalization of SRF with CNPase *in vivo*; during maturation of OLs, CNPase expression is apparent during the transition from OPC to mature OL, followed by MBP and APC expression, with some temporal overlap evident (Scherer et al., 1994, Wada et al., 2000, See et al., 2004). Expression of SRF in APC reactive cells was apparent, but not as abundant as in CNPase positive cells. This may indicate that SRF expression weakens as the cell matures. Furthermore, we have observed a similar phenomenon *in vitro* whereby SRF is strongly upregulated shortly after induction of differentiation; it subsides after several days, but becomes more concentrated in the nucleus. These data are indicative of the close association SRF has with differentiation of OPCs to mature OLs.

Beyond describing the role of SRF in differentiation of OPCs, we have also shown that its expression is controlled by miR-9 and miR-200. We observed that miR-9 and miR-200 are both necessary to inhibit differentiation of OPCs, while miR-200, but not miR-9 could inhibit expression of SRF protein. Co-expression of miR-9 with miR-200 was only modestly more efficacious than miR-200 alone at attenuating SRF expression. Additionally, our luciferase data show that miR-200 likely binds to the *Srf* 3′UTR at only one of two putative binding sites, but that its binding affinity may be stronger than that of miR-9. In our experiments, the miR-9 binding site and the miR-200 binding site that is distal from it, but not the miR-200 binding site proximal to it, showed binding affinity for their respective miRNAs. These data, combined with other reports implicating miR-9 as a negative regulator of OPC differentiation (Lau et al., 2008, Li and Yao, 2012), indicate that miR-9 likely has multiple targets in the gene web that controls differentiation, and that *Srf* is one of those genes. MiR-200 on the other hand may be more specific to *Srf* when expressed in OPCs, given its weaker expression in the CNS, making it a less conspicuous transcript than the abundantly expressed miR-9. There are several other miRNAs including miR-483-5p and miR-122 that have been shown to target 3′UTR of SRF gene (Bai et al., 2009, Qiao et al., 2011). Whether these miRNAs regulate SRF expression in OPCs remains to be investigated, but to date neither has been shown to be altered by ischemic stroke. One limitation of the present study is that our *in vivo* quantitative measurements of miR-9 and miR-200 levels after stroke did not specifically represent OPCs and OLs, although the corpus callosum contains more OPCs and OLs than the striatum and cerebral cortex. However, we suspect that our results would be repeatable in OPCs generally, because we observed strong colocalization of SRF with CNPase in the corpus callosum, striatum and in OPCs of the grey matter, particularly in the cortex.

The present study provides data indicating that miR-9 and miR-200 act at least in part through SRF to regulate maturation of OLs. It is well established that miRNAs play divergent roles in specific cell types or tissues. For example, miR-9 regulates neurogenesis during brain development (Shibata et al., 2011), while miR-200 modulates angiogenesis under hypoxic and wound healing conditions (Chan et al., 2011, Gill et al., 2012). In addition, upregulation of miR-200 by pre-condition ischemia protects ischemic cell damage

(Lee et al., 2010), which may indicate that miR-200 is protective acutely. We and others have demonstrated that stroke induces angiogenesis and neurogenesis (Zhang et al., 2004, Teng et al., 2008). Thus, it is likely that in addition to OPCs, these miRNAs could act on cerebral endothelial and neural progenitor cells in mediating stroke-induced angiogenesis and neurogenesis.

Many transcription factors are involved in differentiation of OPCs. In this study, we have identified a novel transcription factor, SRF, which opens a new avenue of exploration in OPC and stroke research. Axonal sprouting and myelination occur for weeks and months after stroke (Dancause et al., 2005, Liu et al., 2012, Ueno et al., 2012), and SRF may represent a relatively late phase contributor to this natural recovery mechanism. Further studies are warranted to test the effects of elevation of SRF levels—by either overexpression of SRF or downregulation of miR-9 and miR-200—on maturation of OLs *in vivo*, and whether its modulation leads to enhancement of axonal myelination and improvement of neurological outcomes after stroke.

Acknowledgments

This work was supported by National Institute of Neurologic Diseases and Stroke grants PO1 NS23393 (MC), RO1 AG037506 (MC), and RO1 NS075156 (ZGZ) and American Heart Association fellowship 10PRE2730004 (BB). We thank Cynthia Roberts, Deeana Ijaz and Qing-e Lu for technical assistance.

References

Bai S, Nasser MW, Wang B, Hsu SH, Datta J, Kutay H, Yadav A, Nuovo G, Kumar P, Ghoshal K. MicroRNA-122 inhibits tumorigenic properties of hepatocellular carcinoma cells and sensitizes these cells to sorafenib. J Biol Chem. 2009; 284:32015–32027. [PubMed: 19726678]

Buma FE, Lindeman E, Ramsey NF, Kwakkel G. Functional neuroimaging studies of early upper limb recovery after stroke: a systematic review of the literature. Neurorehabil Neural Repair. 2010; 24:589–608. [PubMed: 20439501]

Chan YC, Khanna S, Roy S, Sen CK. miR-200b targets Ets-1 and is down-regulated by hypoxia to induce angiogenic response of endothelial cells. J Biol Chem. 2011; 286:2047–2056. [PubMed: 21081489]

Chen H, Chopp M, Zhang ZG, Garcia JH. The effect of hypothermia on transient middle cerebral artery occlusion in the rat. J Cereb Blood Flow Metab. 1992; 12:621–628. [PubMed: 1618941]

Chen Y, Balasubramaniyan V, Peng J, Hurlock EC, Tallquist M, Li J, Lu QR. Isolation and culture of rat and mouse oligodendrocyte precursor cells. Nat Protoc. 2007; 2:1044–1051. [PubMed: 17546009]

Chida Y, Kokubo Y, Sato S, Kuge A, Takemura S, Kondo R, Kayama T. The alterations of oligodendrocyte, myelin in corpus callosum, and cognitive dysfunction following chronic cerebral ischemia in rats. Brain Res. 2011; 1414:22–31. [PubMed: 21864831]

Dancause N, Barbay S, Frost SB, Plautz EJ, Chen D, Zoubina EV, Stowe AM, Nudo RJ. Extensive cortical rewiring after brain injury. J Neurosci. 2005; 25:10167–10179. [PubMed: 16267224]

Gill JG, Langer EM, Lindsley RC, Cai M, Murphy TL, Murphy KM. Snail promotes the cell-autonomous generation of Flk1 (+) endothelial cells through the repression of the microRNA-200 family. Stem Cells Dev. 2012; 21:167–176. [PubMed: 21861700]

Hayakawa K, Pham LD, Som AT, Lee BJ, Guo S, Lo EH, Arai K. Vascular endothelial growth factor regulates the migration of oligodendrocyte precursor cells. J Neurosci. 2011; 31:10666–10670. [PubMed: 21775609]

Herdegen T, Leah JD. Inducible and constitutive transcription factors in the mammalian nervous system: control of gene expression by Jun, Fos and Krox, and CREB/ATF proteins. Brain Res Brain Res Rev. 1998; 28:370–490. [PubMed: 9858769]

Jurmeister S, Baumann M, Balwierz A, Keklikoglou I, Ward A, Uhlmann S, Zhang JD, Wiemann S, Sahin O. MicroRNA-200c represses migration and invasion of breast cancer cells by targeting

actin-regulatory proteins FHOD1 and PPM1F. Mol Cell Biol. 2012; 32:633–651. [PubMed: 22144583]

Knoll B, Kretz O, Fiedler C, Alberti S, Schutz G, Frotscher M, Nordheim A. Serum response factor controls neuronal circuit assembly in the hippocampus. Nat Neurosci. 2006; 9:195–204. [PubMed: 16415869]

Knoll B, Nordheim A. Functional versatility of transcription factors in the nervous system: the SRF paradigm. Trends Neurosci. 2009; 32:432–442. [PubMed: 19643506]

Lau P, Verrier JD, Nielsen JA, Johnson KR, Notterpek L, Hudson LD. Identification of dynamically regulated microRNA and mRNA networks in developing oligodendrocytes. J Neurosci. 2008; 28:11720–11730. [PubMed: 18987208]

Lee ST, Chu K, Jung KH, Yoon HJ, Jeon D, Kang KM, Park KH, Bae EK, Kim M, Lee SK, Roh JK. MicroRNAs induced during ischemic preconditioning. Stroke. 2010; 41:1646–1651. [PubMed: 20576953]

Li JS, Yao ZX. MicroRNAs: novel regulators of oligodendrocyte differentiation and potential therapeutic targets in demyelination-related diseases. Mol Neurobiol. 2012; 45:200–212. [PubMed: 22218763]

Li Y, McIntosh K, Chen J, Zhang C, Gao Q, Borneman J, Raginski K, Mitchell J, Shen L, Zhang J, Lu D, Chopp M. Allogeneic bone marrow stromal cells promote glial-axonal remodeling without immunologic sensitization after stroke in rats. Exp Neurol. 2006; 198:313–325. [PubMed: 16455080]

Liu Z, Li Y, Zhang L, Xin H, Cui Y, Hanson LR, Frey WH 2nd, Chopp M. Subacute intranasal administration of tissue plasminogen activator increases functional recovery and axonal remodeling after stroke in rats. Neurobiol Dis. 2012; 45:804–809. [PubMed: 22115941]

Liu Z, Li Y, Zhang ZG, Cui X, Cui Y, Lu M, Savant-Bhonsale S, Chopp M. Bone marrow stromal cells enhance inter- and intracortical axonal connections after ischemic stroke in adult rats. J Cereb Blood Flow Metab. 2010; 30:1288–1295. [PubMed: 20125183]

Livak KJ, Schmittgen TD. Analysis of relative gene expression data using real-time quantitative PCR and the 2(−Delta Delta C (T)) Method. Methods. 2001; 25:402–408. [PubMed: 11846609]

Lu PP, Ramanan N. A critical cell-intrinsic role for serum response factor in glial specification in the CNS. J Neurosci. 2012; 32:8012–8023. [PubMed: 22674276]

Lu Y, Zhang Y, Shan H, Pan Z, Li X, Li B, Xu C, Zhang B, Zhang F, Dong D, Song W, Qiao G, Yang B. MicroRNA-1 downregulation by propranolol in a rat model of myocardial infarction: a new mechanism for ischaemic cardioprotection. Cardiovasc Res. 2009; 84:434–441. [PubMed: 19581315]

Lyons SA, Kettenmann H. Oligodendrocytes and microglia are selectively vulnerable to combined hypoxia and hypoglycemia injury in vitro. J Cereb Blood Flow Metab. 1998; 18:521–530. [PubMed: 9591844]

McIver SR, Muccigrosso M, Gonzales ER, Lee JM, Roberts MS, Sands MS, Goldberg MP. Oligodendrocyte degeneration and recovery after focal cerebral ischemia. Neuroscience. 2010; 169:1364–1375. [PubMed: 20621643]

Morris DC, Chopp M, Zhang L, Zhang ZG. Thymosin beta4: a candidate for treatment of stroke? Ann N Y Acad Sci. 2010; 1194:112–117. [PubMed: 20536457]

Paez PM, Garcia CI, Davio C, Campagnoni AT, Soto EF, Pasquini JM. Apotransferrin promotes the differentiation of two oligodendroglial cell lines. Glia. 2004; 46:207–217. [PubMed: 15042587]

Pantoni L, Garcia JH, Gutierrez JA. Cerebral white matter is highly vulnerable to ischemia. Stroke. 1996; 27:1641–1646. discussion 1647. [PubMed: 8784142]

Qiao Y, Ma N, Wang X, Hui Y, Li F, Xiang Y, Zhou J, Zou C, Jin J, Lv G, Jin H, Gao X. MiR-483-5p controls angiogenesis in vitro and targets serum response factor. FEBS Lett. 2011; 585:3095–3100. [PubMed: 21893058]

Riechmann JL, Meyerowitz EM. MADS domain proteins in plant development. Biol Chem. 1997; 378:1079–1101. [PubMed: 9372178]

Saur D, Lange R, Baumgaertner A, Schraknepper V, Willmes K, Rijntjes M, Weiller C. Dynamics of language reorganization after stroke. Brain. 2006; 129:1371–1384. [PubMed: 16638796]

Scherer SS, Braun PE, Grinspan J, Collarini E, Wang DY, Kamholz J. Differential regulation of the 2′, 3′-cyclic nucleotide 3′-phosphodiesterase gene during oligodendrocyte development. Neuron. 1994; 12:1363–1375. [PubMed: 8011341]

See J, Zhang X, Eraydin N, Mun SB, Mamontov P, Golden JA, Grinspan JB. Oligodendrocyte maturation is inhibited by bone morphogenetic protein. Mol Cell Neurosci. 2004; 26:481–492. [PubMed: 15276151]

Shen LH, Li Y, Chen J, Zhang J, Vanguri P, Borneman J, Chopp M. Intracarotid transplantation of bone marrow stromal cells increases axon-myelin remodeling after stroke. Neuroscience. 2006; 137:393–399. [PubMed: 16298076]

Shibata M, Nakao H, Kiyonari H, Abe T, Aizawa S. MicroRNA-9 Regulates Neurogenesis in Mouse Telencephalon by Targeting Multiple Transcription Factors. J Neurosci. 2011; 31:3407–3422. [PubMed: 21368052]

Shore P, Sharrocks AD. The MADS-box family of transcription factors. Eur J Biochem. 1995; 229:1–13. [PubMed: 7744019]

Smirnova L, Grafe A, Seiler A, Schumacher S, Nitsch R, Wulczyn FG. Regulation of miRNA expression during neural cell specification. Eur J Neurosci. 2005; 21:1469–1477. [PubMed: 15845075]

Stritt C, Stern S, Harting K, Manke T, Sinske D, Schwarz H, Vingron M, Nordheim A, Knoll B. Paracrine control of oligodendrocyte differentiation by SRF-directed neuronal gene expression. Nat Neurosci. 2009; 12:418–427. [PubMed: 19270689]

Teng H, Zhang ZG, Wang L, Zhang RL, Zhang L, Morris D, Gregg SR, Wu Z, Jiang A, Lu M, Zlokovic BV, Chopp M. Coupling of angiogenesis and neurogenesis in cultured endothelial cells and neural progenitor cells after stroke. J Cereb Blood Flow Metab. 2008; 28:764–771. [PubMed: 17971789]

Ueno Y, Chopp M, Zhang L, Buller B, Liu Z, Lehman NL, Liu XS, Zhang Y, Roberts C, Zhang ZG. Axonal Outgrowth and Dendritic Plasticity in the Cortical Peri-Infarct Area After Experimental Stroke. Stroke. 2012

Wada T, Kagawa T, Ivanova A, Zalc B, Shirasaki R, Murakami F, Iemura S, Ueno N, Ikenaka K. Dorsal spinal cord inhibits oligodendrocyte development. Dev Biol. 2000; 227:42–55. [PubMed: 11076675]

Wang LE, Tittgemeyer M, Imperati D, Diekhoff S, Ameli M, Fink GR, Grefkes C. Degeneration of corpus callosum and recovery of motor function after stroke: A multimodal magnetic resonance imaging study. Hum Brain Mapp. 2011

Zhang J, Li Y, Zhang ZG, Lu M, Borneman J, Buller B, Savant-Bhonsale S, Elias SB, Chopp M. Bone marrow stromal cells increase oligodendrogenesis after stroke. J Cereb Blood Flow Metab. 2009; 29:1166–1174. [PubMed: 19384336]

Zhang J, Li Y, Zheng X, Gao Q, Liu Z, Qu R, Borneman J, Elias SB, Chopp M. Bone marrow stromal cells protect oligodendrocytes from oxygen-glucose deprivation injury. J Neurosci Res. 2008; 86:1501–1510. [PubMed: 18214988]

Zhang L, Chopp M, Zhang RL, Wang L, Zhang J, Wang Y, Toh Y, Santra M, Lu M, Zhang ZG. Erythropoietin amplifies stroke-induced oligodendrogenesis in the rat. PLoS One. 2010; 5:e11016. [PubMed: 20552017]

Zhang R, Zhang Z, Wang L, Wang Y, Gousev A, Zhang L, Ho KL, Morshead C, Chopp M. Activated neural stem cells contribute to stroke-induced neurogenesis and neuroblast migration toward the infarct boundary in adult rats. J Cereb Blood Flow Metab. 2004; 24:441–448. [PubMed: 15087713]

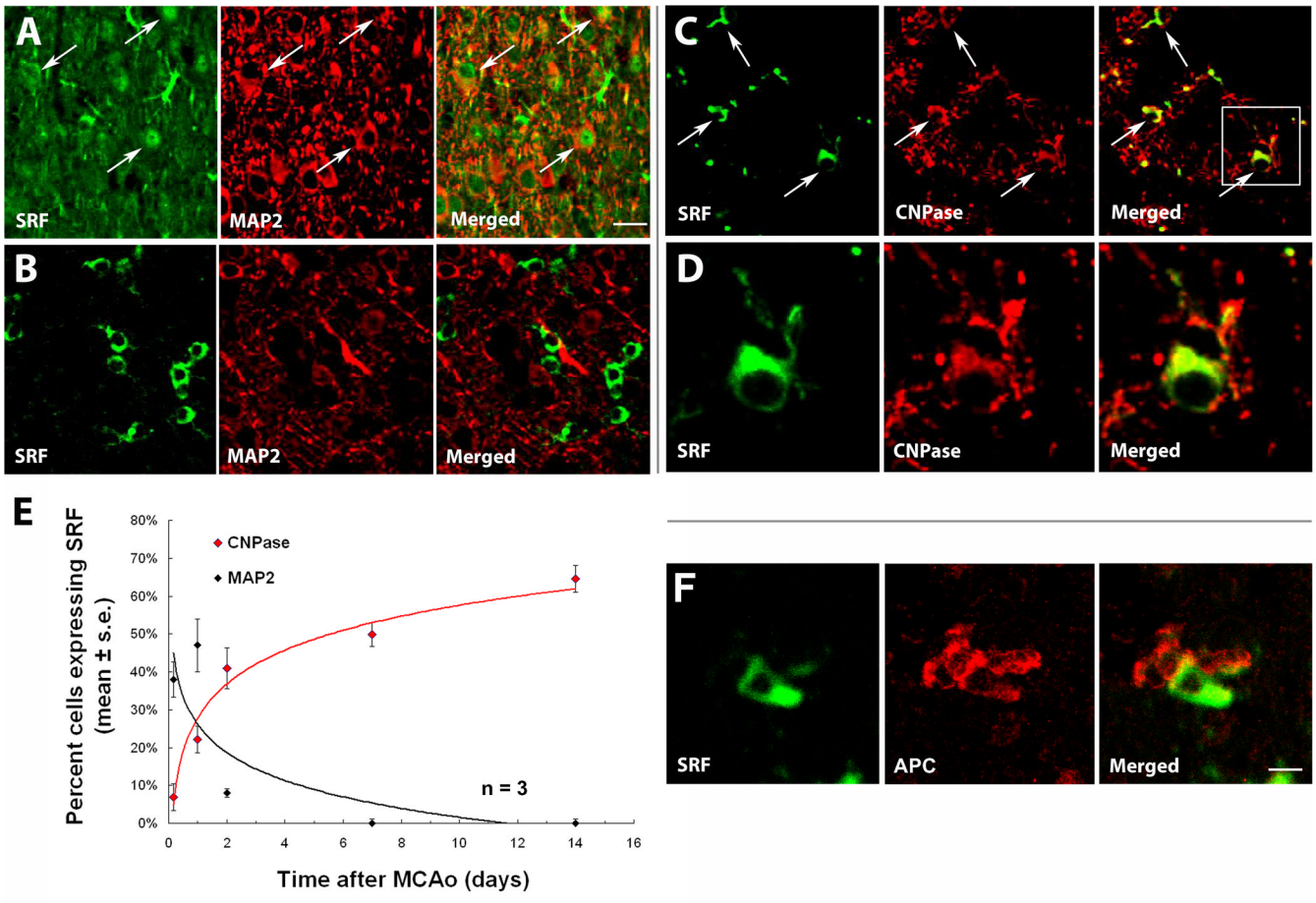

Figure 1.

Confocal immunofluorescent images show that SRF colocalizes with distinct cell populations at different times after stroke. Four hours after the onset of ischemia, many SRF positive cells (A, green, arrows) were also MAP2 positive (A, red, arrows). Fourteen days after stroke, SRF positive cells (B and C, green) were no longer MAP2 positive (B, red), but were CNPase positive (C, red, arrows). Higher magnification images of the boxed area in C show colocalization of SRF (D, green) and CNPase (D, red). Panel E shows quantification of SRF immunoreactivity in MAP2 and CNPase positive cells. n = 3 per time point. At 14d after stroke, SRF colocalizes with APC in the IBZ (F), but its expression is weaker than in CNPase cells. Scale bar: A, B, C = 20μm; D = 7μm; F= 5μm.

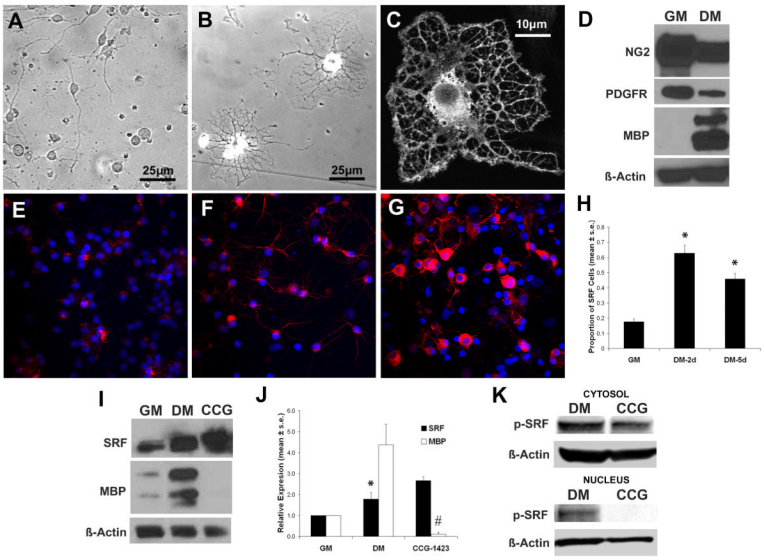

Figure 2.

SRF activity regulates MBP levels. Light microscopic images (A and B) show typical morphology of the OPCs cultured in the GM and DM, respectively, the former having fewer, longer processes, and the latter a highly branched morphology; cells in DM for several days express MBP highly, as shown by anti-MBP immunofluorescence (C), and a representative Western blot (D) reveals other maturity markers. Representative immunofluorescent images show SRF (red; blue = DAPI) positive cells in GM (E) and DM for 2 (F) and 5 (G) days, with quantitative data in (H). A representative Western blot and quantitative analysis of Western blot data show SRF and MBP levels of the OPCs in the GM, DM or DM with an SRF inhibitor, CCG-1423 (I, J). Panel (K) shows cytosol and nucleus protein levels of p-SRF in OPCs treated with CCG-1423. CCG-1423 = 300 nM CCG-1423 added toDM. *P < 0.05 vs. GM; #P < 0.05 vs. DM.

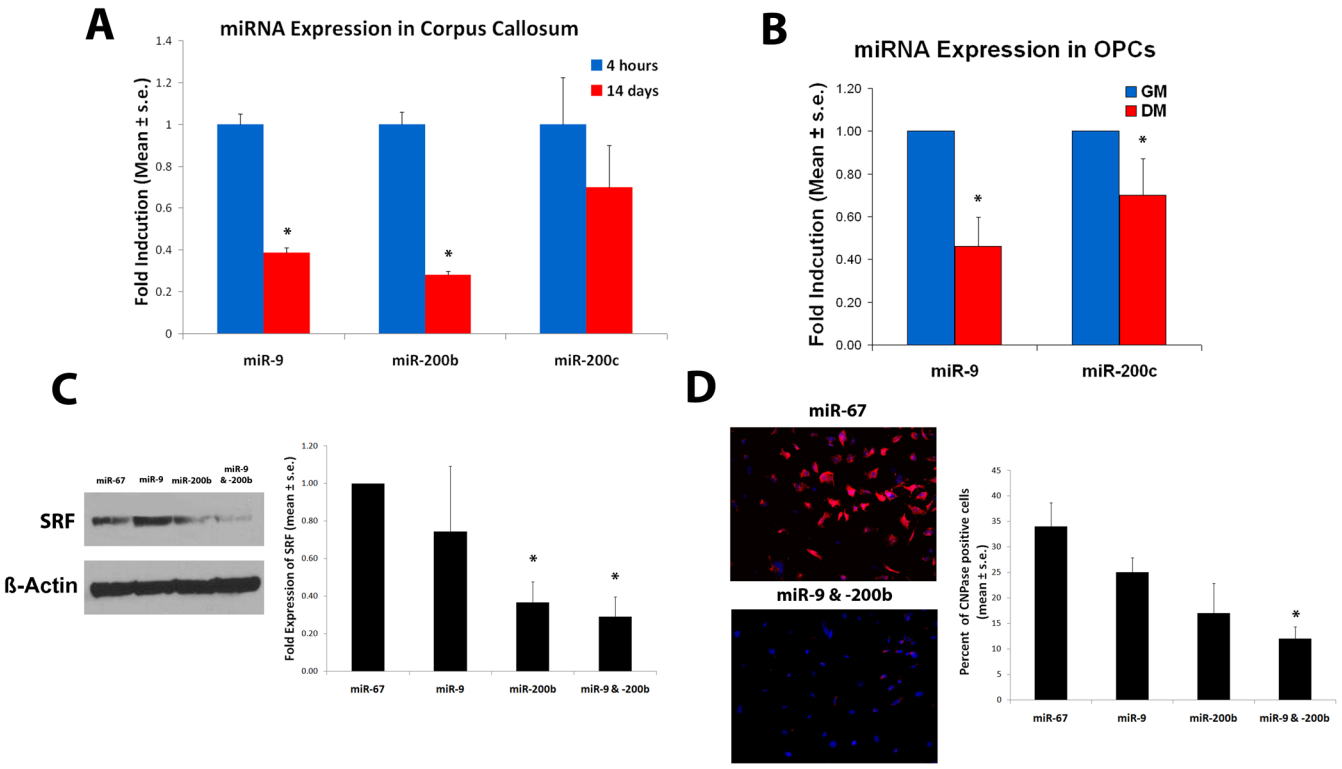

Figure 3.

MiR-9 and miR-200 regulate expression of SRF. Real-time RT-PCR analysis shows levels of miR-9, miR-200b and miR-200c in the ipsilateral corpus callosum 4h and 14d after stroke (A, n = 5/group) and in the primary OPCs cultured in DM and GM (B, n = 3/group). Western blot analysis (C, n = 3) shows SRF levels in N20.1 cells overexpressed with miR-67, miR-200b, miR-9, or miR-200b and miR-9. Immunocytochemistry analysis (D, n = 4) shows CNPase immunoreactive cells (red) in N20.1 cells overexpressed with miR-67, miR-200b, miR-9, or miR-200b and miR-9. Blue color = DAPI positive nuclei; miR-67 was used as control. *P < 0.05

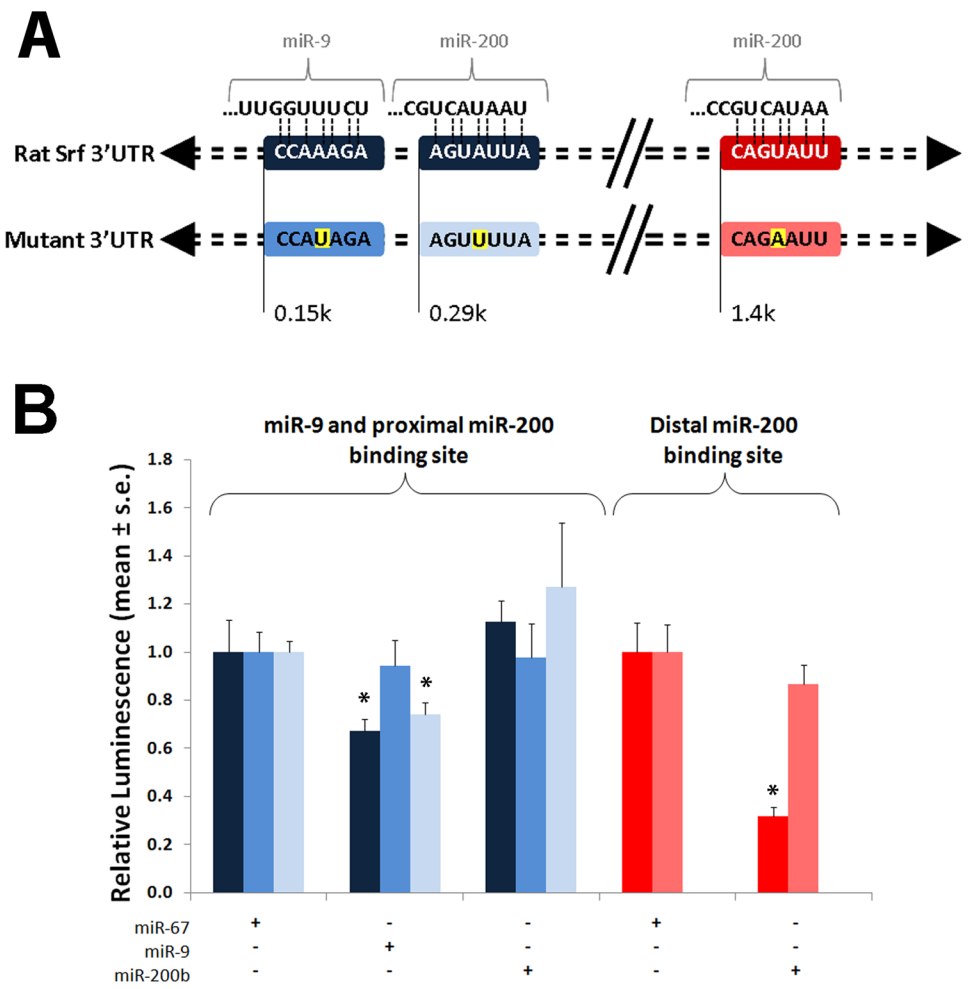

Figure 4.

MiR-9 and miR-200 target *Srf*. A carton (A) shows alignment of seed sequences of rat miR-9 and miR-200 and potential miR-9 and miR-200 proximal (blue) and distal (red) binding sites in the *Srf* 3′UTR. The miRNA and mRNA sequences shown are exactly homologous in Rat and Human. Yellow boxes in the seed sequences of miR-9 and miR-200 indicate an altered nucleotide (A, Mutant). N20.1 cells were transfected with pMiR report luciferase vector containing either wild-type or mutated SRF 3′UTR (B). Relative luciferase activity was standardized to a miR-67 control. The colored bars in panel B correspond to the colors highlighting each sequence in panel A. MiR-9, miR-200 or miR-67 were co-expressed with each assay, indicated by + or − below each bar. n = 4; *P < 0.05